ISSN : 0974 - 7443 Volume 8 Issue 1

CHEMICAL TECHNOLOGY

An Indian Journal

Full Paper

Trade Science Inc.

CTAIJ 8(1) 2013 [17-27]

Modeling a non-ideal VGO hydrocracking reactor using selective overall effectiveness factors

Sepehr Sadighi

Reaction Engineering Department, Catalysis Research Center and Nano Technology, Research Institute of Petroleum Industry, Tehran, (IRAN)

E-mail: sadighis@ripi.ir

ABSTRACT

The reported pilot experiments in the previous work were used to develop an optimized model for a pilot scale hydrocracker of vacuum gas oil (VGO) under the following reaction conditions: temperature from 380°C to 420°C, pressure of 156 bar, hydrogen-to-oil ratio of 1780 Nm^3/Sm^3 and liquid hourly space velocity (LHSV) ranging from 0.5 to 2 hr^{-1}. A commercial dual functional amorphous catalyst was used in all experiments. The product of the reactor based on the most value added products was characterized to dry gas, light naphtha, heavy naphtha, kerosene, diesel and unconverted VGO. At first, a six-lump discrete lumping network including fifteen reactions was developed for the prediction of hydrocracking product yields. After applying the weighted lumping strategy, reducing the kinetic network and using selective effectiveness factors, the absolute average deviation (*AAD%*), R-squared and F-test of the model were reduced from 57.17%, 93.69% and 32.1 to 35.01%, 94.58% and 69.7, respectively. Then, to model the axial-dispersion effect through the catalytic bed, the N-tanks in series approach was used which could be shifted from plug ideal-flow regime (N=200) to complete mixed flow regime (N=1), according to the Fibonacci series, to increase the accuracy of the model. Results confirmed that the best value for the number of series tanks, searched by Fibonacci golden numbers, was thirteen which reduced the final *AAD%*, R-squared and F-test of the predicted yields to 31.59%, 95.15% and 73.6, respectively. Additionally, the estimated overall effectiveness factors by experimental data agree with the molecular diffusion and transport phenomena during hydrocracking process.

KEYWORDS

Hydrocracking;
Modeling;
Weighted lumping;
Effectiveness factor;
Non-ideal flow.

INTRODUCTION

Petroleum refining is now in a significant transition period as the industry has moved into the 21st century and the demand for petroleum products has shown a sharp growth in recent years, especially with the recent entry of China into the automobile market. This means that the demand transportation fuels will show a steady growth in the next decade, contributing to petroleum product demand patterns that can only be fulfilled by the inclusion of heavier feedstock into refinery operations[12]. This heavy feedstock can be converted to lighter ones using thermal and/or catalytic processing in the absence or presence of hydrogen pressure[19,10].

Full Paper

Hydrocracking is one of the most versatile of all petroleum-refining processes which is the most attractive process for production of clean transportation fuels, for example, diesel with high quality[11].

Needed for all industrial processes, the optimal operation is required to guarantee the profitability which can be achieved by process models. These models are used to predict the product yields and qualities, and they are useful for sensitivity analysis, process optimization, and control, design of new plants and selection of suitable hydrocracking catalysts. However, the complexity of hydrocracking feed makes it extremely difficult to characterize and describe its kinetic at a molecular level which can be solved by considering the partition of the species into a few equivalent classes, the so-called lumps or lumping technique, and then assume each class is an independent entity. As it is mentioned in literatures, developing simple kinetic models (e.g., power-law model) for complex catalytic reactions is a common approach as it can give basic information for catalyst screening, reactor design and optimization. In this field, many works were reported in literatures[1,3-7,23,26-28]. In all of these works, the hydrocracking reactor was assumed in a plug flow regime.

In a different approach[14], to simulate the non-ideal behavior of the flow regime through reactor, the description of the hydrocracking kinetic of Kuwait VGO feed was done according to TBP distribution curve and an axial-description kinetic model.

The present study was aimed at developing an improved kinetic model, according to a six-lump approach, to predict the most added value products including gas (lights and LPG), light naphtha, heavy naphtha, kerosene and diesel in a pilot scale hydrocracking reactor, which its feed was vacuum gas oil (VGO). The advantages of this work were: I) by using selective factors, called overall effectiveness factors which were estimated from experimental data, the accuracy of the yield prediction was increased, and II) for the reason of existing non-idealities, a N-series tanks kinetic model was applied to increase the accuracy of the yield prediction in comparison to an ideal plug flow assumption that the best value for the number of tanks (N) was found by Fibonacci golden numbers.

EXPERIMENTAL DATA

The required model parameters were estimated from the sixteen pilot plant data for hydrocracking vacuum gas oil (VGO) reported in the previous work[27] in which hycrocracking was performed under the following conditions: 1. $H_2/HC = 1780\ Nm^3/Sm^3$; 2. LHSV = 0.5, 1, 1.5 and 2 hr^{-1}; 3. Temperature = 380, 400, 410 and 420 ^oC, and 4. Pressure = 156 bar.

To do the experiments, the reactor bed was loaded with 33 g (50 cm^3) of a dual functional amorphous catalyst. The mesh of the catalyst particles was 10-20 (0.83-1.65 mm). The internal diameter of the reactor was about 1 inch.

As a rule, for examining the importance of axial mixing, a useful parameter is the ratio L/d_p, where L is the length of the bed and d_p is the diameter of the catalyst particle. The ratio D/d_p, where D is the internal diameter of the reactor, is also frequently used. Thus, a widely accepted empirical criterion is used to design experimental setup or to determine if axial mixing can be neglected[17] and is given as the following:

$$\frac{L}{d_p} \geq 100 \quad \text{and} \quad \frac{D}{d_p} \geq 10 \qquad (1)$$

According to the presented data for the understudy reactor, the length of the reactor bed was about (10 cm). Therefore the length of the bed to catalyst particle diameter was ranging from 59.8 to 118.5 which implied the possibility of the axial-dispersion phenomenon thorough the catalytic bed.

HYDROCRACKING REACTION NETWORK

This work presented six lumps, i.e. unconverted VGO or residue, diesel, kerosene, light naphtha, heavy naphtha and gas to predict all valuable products of pilot plant reactor. Figure 1 depicts the reaction pathways associated with this strategy. Note that if all reaction pathways were considered, the model including thirty kinetic parameters (frequency factors and apparent activation energies) which should be estimated using experimental data and it was laborious. Some judgments were normally welcome to reduce the model complexity, without scarifying the accuracy[26-28].

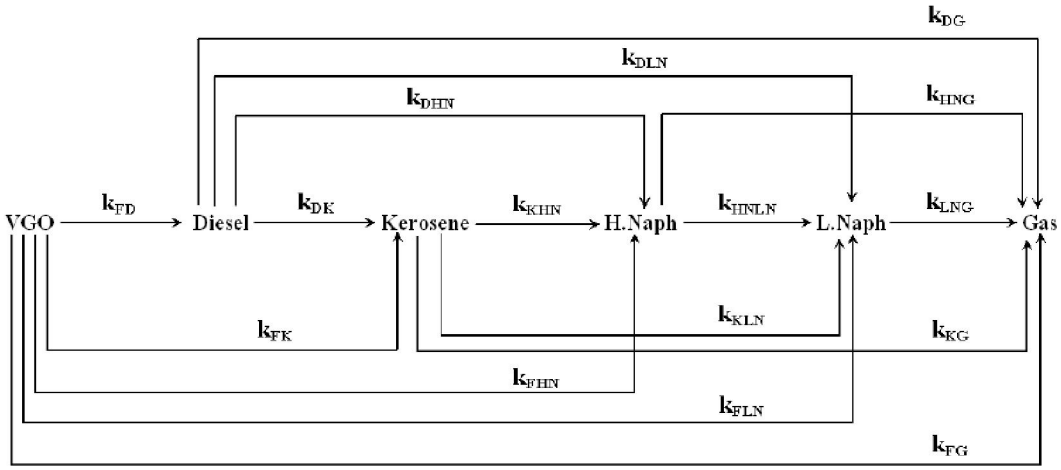

Figure 1 : The complete six-lump kinetic model.

In Figure 1, k, F, D, K, HN, LN and G demonstrate rate constant, VGO feed, diesel, kerosene, heavy naphtha, light naphtha and gas respectively. The combination of these nominators, show the path of hydrocracking reaction. For example, k_{FD} represents the rate constant for conversion VGO feed to diesel.

MODELING APPROACH

Mathematical models for the VGO hydrocracking process, in a trickle-bed regime, can be very complex due to the many microscopic and macroscopic effects occurring inside the[25]. So, some assumptions were introduced to simplify the model as follows

1- Hydrocracking was a first order hydrocracking reaction[21]. Since hydrogen was present in excess, the rate of hydrocracking can be supposed to be independent of the hydrogen concentration.
2- The pilot reactor operated under isothermal conditions.
3- Hydrogen feed was pure.
4- The feed and products were in the liquid phase.
5- The operation of the pilot unit was steady state.
6- Catalyst activity did not change with time. Hence simulation was only valid for the start of run.

For each reaction, a kinetic expression (*R*) was formulated as a function of mass concentration (*C*) and kinetic parameters (k_0,*E*).

Based on these assumptions, the kinetic constants of proposed model were as the following.

Vacuum gas oil or Feed (*F*):

$$\mathbf{k_{Fj} = k_{0Fj}\, exp(\frac{-E_{Fj}}{RT})} \qquad \mathbf{(2)}$$

Note that *j* in Eq. (1) represents diesel (*D*), kerosene (*K*), heavy naphtha (*HN*), light naphtha (*LN*) and gas (*G*) lumps.

Diesel (*D*):

$$\mathbf{k_{Dj'} = k_{0Dj'}\, exp(\frac{-E_{Dj'}}{RT})} \qquad \mathbf{(3)}$$

j' in Eq. (2) represents kerosene (*K*), heavy naphtha (*HN*), light naphtha (*LN*) and gas (*G*) lumps.

Kerosene (*K*):

$$\mathbf{k_{Kj''} = k_{0Kj''}\, exp(\frac{-E_{Kj''}}{RT})} \qquad \mathbf{(4)}$$

j'' in Eq. (3) are heavy naphtha (*HN*), light naphtha (*LN*) and gas (*G*) lumps.

Heavy Naphtha (*HN*):

$$\mathbf{k_{HNj'''} = k_{0HNj'''}\, exp(\frac{-E_{HNj'''}}{RT})} \qquad \mathbf{(5)}$$

j''' in Eq. (4) are light naphtha (*LN*) and gas (*G*) lumps.

Light Naphtha (*LN*):

$$\mathbf{k_{LNG} = k_{0LNG}\, exp(\frac{-E_{LNG}}{RT})} \qquad \mathbf{(6)}$$

In Eqs. (2) to (6), *T* and *R* are the absolute value of bed temperature and ideal gas constant, respectively.

The reaction rates (*R*) can be formulated as the following.

Vacuum gas oil reaction (R_F):

$$\mathbf{R_F = \sum_{j=D}^{G} \eta_F k_{Fj} C_F} \qquad \mathbf{(7)}$$

Diesel (R_D):

$$\mathbf{R_D = \eta_F k_{FD} C_F - \sum_{j'=K}^{G} \eta_D k_{Dj'} C_D} \qquad \mathbf{(8)}$$

Full Paper

Kerosene (R_K):

$$R_K = \eta_F k_{FK} C_F + \eta_D k_{DK} C_D - \sum_{j''=HN}^{G} \eta_K k_{Kj''} C_K \quad (9)$$

Heavy Naphtha (R_{HN}):

$$R_{HN} = \eta_F k_{FHN} C_F + \eta_D k_{DHN} C_D + \eta_K k_{KHN} C_K - \sum_{j'''=LN}^{G} \eta_{HN} k_{HNj'''} C_{HN} \quad (10)$$

Light Naphtha (R_{LN}):

$$R_{LN} = \eta_F k_{FLN} C_F + \eta_D k_{DLN} C_D + \eta_K k_{KLN} C_K + \eta_{HN} k_{HNLN} C_{HN} - \eta_{LN} k_{LNG} C_{LN} \quad (11)$$

Gas (R_G):

$$R_G = \eta_F k_{FG} C_F + \eta_D k_{DG} C_D + \eta_K k_{KG} C_K + \eta_{HN} k_{HNG} C_{HN} + \eta_{LN} k_{LNG} C_{LN} \quad (12)$$

where η_D, η_K, η_{HN} and η_{LN} are the overall effectiveness factors for the VGO, diesel, kerosene, heavy naphtha and light naphtha lumps, respectively, which is supposed to import the effects of the mass and pore diffusion resistance in the model. These factors can be affected by the external catalyst wetting and fractional pore filling in trickle-bed reactors. It is obvious that these factors are different for each lump. The effectiveness factor in the trickle bed regime for a spherical catalyst for an external contacting efficiency of 0.5 and Thiele modulus of 50 was calculated ranging from 0.83 to 0.8[20]. In this research, selective effectiveness factors for the hydrocracking reactions were considered which were estimated from experimental data during parameter estimation. Regardless to the phenomena which could affect the introduced effectiveness factors in this work, they were estimated such as model parameters to minimize the least square objective function (Eq. 19), presented in the next section.

Mass balance equations

Plug flow for fixed-bed reactors was assumed in many reported models in literature, consisting of a set of ordinary differential equation (ODEs) with defined boundary conditions. In this paper, to model the hydrocracking reactor, a cell network approach was used which its accuracy was confirmed for trickle bed reactors[13]. As shown in Figure 3, the hydrocracking section from the inlet to the outlet was visualized to be divided into a number of well-mixed cells (N=200 for plug flow regime) along the longitude direction. Mixing only occurred within each cell and back mixing was not accounted for the adjacent cells. The main advantage of the aforesaid approach was that the solution of ordinary differential equations was converted into the solution of a set of algebraic equations for a hydrocracking process which needed less time, and it was mathematically stable.

Decreasing the number of series tanks can simulate the reverse effect of axial-dispersion, along the reactor bed. The optimized value can be searched from 200 to 1 (N=1 shows a complete mixed flow regime) according to the Fibonacci series or golden numbers which are (N=144, 89, 55, 34, 21, 13, 8, 5, 3, 2, 1)[9]. This approach was equivalent to a one-parameter non-ideal reactor model[16] that was adopted in some of the previous works in reactor modeling[15,24].

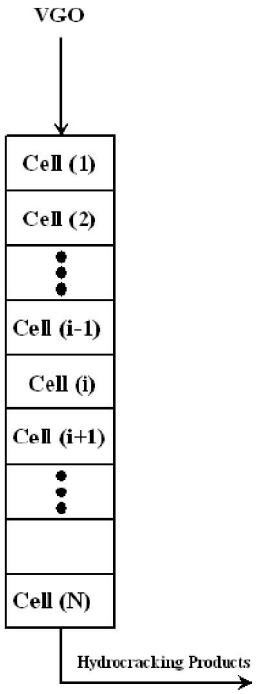

Figure 2 : Schematic representation of series mixed cells.

The overall mass balance equations for all lumps are expressed as

$$C_j(i-1)\nu(i-1) \pm .\varepsilon'.R_j(i) \times Vcat(i) = C_j(i)\nu(i) \quad (13)$$

Here, the "-" is for reactant (feed or VGO), and the "+" sign is for the products.

$$\upsilon(i) = \frac{F_m(i)}{\rho(i)} \quad (14)$$

$$F_m(i) = \sum_{j=F}^{G} C_j(i)\upsilon(i) \quad (15)$$

$$Y_j = \frac{C_j.\upsilon(i)}{F_m(i)} \quad (16)$$

$$V_{cat}(i) = \frac{V_b}{N} \quad (17)$$

where ε' is catalyst volume fraction; V_b is catalyst bed volume; F_m is feed mass flow rate ; C_j is lumps mass concentration; v is volume flow rate through reactor; Y_j is product yield and ρ is the density of stream through reactor. The catalyst volume fraction for this work was about 0.264.

The only remained unknown variable is the density of the stream inside the reactor ρ which can be calculated as follows.

$$\frac{1}{\rho_0} = \sum_{j=F}^{G} \frac{Y_j}{\rho_j} \quad (18)$$

Where, ρ_j is the density of each lump.

The reaction and mass balance expressions according to Eq. 2 to Eq. 18 were solved simultaneously to evaluate the product yields (Y_i) by using Aspen Custom Modeler (ACM) programming environment (AspenTech, 2004).

Parameter estimation

For the parameter estimation two methods were used as follows:

(a) Un-weighted method

In this method, the sum of squared error, SQE_1, as given below, was minimized whilst all weight function (w_j) were one.

$$SQE_1 = \sum_{n=1}^{N_t} \sum_{j=F}^{G} w_j.(Y_{nj}^{meas} - Y_{nj}^{pred})^2 \quad (19)$$

where N_t, Y_{kj}^{meas} and Y_{kj}^{pred} were the number of test runs, measured yield and the predicted one, respectively.

(b) Weighted method

Before minimizing Eq. 19, the weight functions (w) were determined by minimizing the following expression[28]:

$$SQE_2 = \sum_{j=G}^{F} (w_j \sum_{n=1}^{N_t} Y_{nj} - w_{ref} \sum_{n=1}^{N_t} Y_{ref})^2 \quad (20)$$

$$\text{Subject to } w_{j,ref} > 0$$

where w_j in Eq. 20 was the weight coefficient of lumps, which played a crucial role to have an evenly distributed *AAD%* along the predicted yield for the lump with higher yield like diesel and the lump with lower yield like light naphtha[28]. The subscript *ref* in Eq. 20 refers to the lump with the lowest yield which was light naphtha in this work.

At first, in order to estimate weight parameters, the objective function presented in Eq. 20 was minimized by solver tool in Excel package by using Newton search method. Then Eq. 19 was minimized by applying these weights and sequencing NL2Sol and Nelder-mead algorithm, which were available in Aspen Custom Modeler software. To promote convergence from a poor initial point, a trust, the approximate region was found with NL2Sol; then to fine tune the parameters; Nelder-Mead simplex method was used.

The adequacy of the simulated yields was checked with an analysis of variance (ANOVA) using R-squared and the Fischer F-test with a 1% critical level[8,22]. Additionally, to compare the simulated and measured product values, the absolute average deviation (AAD%) was expressed as[26]:

$$AAD\% = 100 \frac{\sum_{n=1}^{N_t} \sum_{j=F}^{G} \sqrt{\frac{(Y_{jn}^{meas} - Y_{jn}^{pred})^2}{Y_{jn}^{meas\,2}}}}{N_t}\% \quad (21)$$

RESULTS AND DISCUSSION

Plug ideal-flow regime

At first, it was assumed that the flow regime of the reactor was an ideal plug one. Therefore, the number of series tanks was set to 200. The kinetic parameters of the model were estimated by the following strategies:

(a) Complete un-weighted strategy (200C)

In this strategy, it was assumed that all reaction pathways presented in Figure 1 were activated by the catalyst. Moreover, the overall effectiveness factors for all lumps were considered equal to 0.8. After estimating the kinetic parameters, the AAD%, R-squared and F-test of the model prediction were calculated and demonstrated with the title of 200C in the Figures 4, 5 and

6, respectively.

(b) Complete weighted strategy (200W)

The next try for parameter estimation was done by using the factors presented in TABLE 1, which were estimated from minimizing of Eq. 20. After applying these weight parameters in Eq. 19, AAD%, R-squared and F-test of the model prediction were calculated and demonstrated with the title of 200W in the Figures 4, 5 and 6, respectively.

TABLE 1 : Estimated factors for weighted estimation.

Lump	Weight factor
Gas	0.2
Light Naphtha	1.56
Heavy Naphtha	0.39
Kerosene	0.15
Diesel	0.11
Un.VGO	0.08

TABLE 2 : Kinetic parameters for the complete-unweighted network.

Frequency Factor k_0[$m^3.hr^{-1}.m^{-3}$ cat^{-1}]		Activation Energy E [kcal/mol]		Rate k_o exp ($-E/RT_{mean}$)	Order (to k_{LNG})
k_{0FD}	3.71×10^{5}	E_{FD}	15.46	3.69	0.139
k_{0Fk}	9.02×10^{6}	E_{Fk}	20.83	1.63	0.062
k_{0FHN}	2.75×10^{1}	E_{FHN}	30.71	3.17×10^{-9}	1.19×10^{-10}
k_{0FLN}	1.08×10^{6}	E_{FLN}	19.69	0.45	0.017
k_{0FG}	8.75×10^{6}	E_{FG}	21.92	7.03×10^{-1}	0.027
k_{0DK}	1.70×10^{6}	E_{DK}	17.54	3.57	0.135
k_{0DHN}	5.58×10^{3}	E_{DHN}	43.32	5.3×10^{-11}	2.01×10^{-12}
k_{0DLN}	3.04×10^{-3}	E_{DLN}	24.43	3.77×10^{-11}	1.42×10^{-12}
k_{0DG}	4.62×10^{3}	E_{DG}	39.33	8.61×10^{-10}	3×10^{-11}
k_{0KHN}	2.73×10^{5}	E_{KHN}	14.87	4.20	0.159
k_{0KLN}	5.20×10^{-2}	E_{KLN}	45.48	9.92×10^{-17}	4×10^{-18}
k_{0KG}	6.24×10^{-2}	E_{KG}	23.42	1.64×10^{-9}	6×10^{-11}
k_{0HNLN}	1.70×10^{3}	E_{HNLN}	7.74	5.34	0.202
k_{0HNG}	1.83×10^{-3}	E_{HNG}	7.54	6.64×10^{-6}	2.5×10^{-7}
k_{0LNG}	2.65×10^{1}	E_{LNG}	0	26.48	1

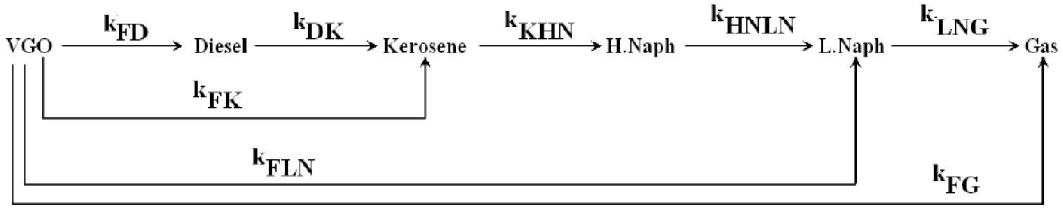

Figure 3 : The reduced six-lump kinetic model.

It can be understood from Figures 4, 5 and 6 that the AAD%, R-squared and F-test of the model prediction resulted by the complete weighted strategy (200W) were considerably better than the complete un-weighted strategy (200C) which confirmed the validity of the weighted lumping strategy, as it was discussed in the previous work for a five-lump reaction network[28].

TABLE 2 shows the estimated values of apparent activation energies and frequency factors by the complete weighted strategy. In this table, the rate constants for all reactions were evaluated in the average operating temperature (402.5^{0}C). Moreover, it shows that the paths including feed to heavy naphtha, diesel to heavy naphtha, diesel to light naphtha, diesel to gas, kerosene to light naphtha, kerosene to gas and heavy naphtha to gas are ignorable due to low constant rates. Moreover, in the operating temperatures, the rate of light naphtha to gas is independent to the temperature; therefore its activation energy can be ignored. These phenomena have been discussed in the previous works[26-28]. In order to reduce the number of kinetic parameters involved in the model, the mentioned constants can be omitted during parameter estimation. Now, fifteen remained kinetic parameters should be estimated by ninety-six observations, creating more acceptable degree of freedom. After eliminating the least possible reactions, the reduced reaction network is depicted in Figure 3.

Although activation energies for the hydrocracking process are strongly related to the type of both feed and catalyst, the estimated values in this work were nevertheless comparable found in previous studies. As revealed by TABLE 2, the apparent activation energy of VGO hydrocracking to middle distillate and naphtha are about 15-21 kcal/mol and 19-31 kcal/mol, respectively. The reported ones by Aboul-Ghiet[1] for hydrocracking of VGO to middle distillate and naphtha were about 13-17.5 kcal/mol and 22-24 kcal/mol, respectively, not far from this research. Furthermore, the activation energy of catalytic cracking of naphtha to gas, reported by Ancheyta et al.[2] was 9-9.92 kcal/mol, close to the reported one for heavy naphtha in this work.

Moreover, the apparent activation energies for the cracking of feed to kerosene and heavy naphtha to light naphtha found in this work are close to those reported in the previous work[26], at 15.87 and 11.59 kcal/mol, respectively. All estimated activation energies in this paper are lower than reported values by Sanchez et al.[3] for a 5-lump model. It seems because VGO feed in Sanchez work was the product of heavy residue, its cracking to lighter lumps needs higher activation energy than the lighter VGO used in this current work.

(c) Reduced weighted strategy (200WR)

The kinetic parameters of the reduced model were estimated again by using measured data, producing new model predictions. Upon comparing the measured data with the model predictions, the AAD%, R-squared and F-test of the model prediction were calculated and demonstrated with the title of 200WR in the Figures 4, 5 and 6, respectively. Similar to the previous works[26-28], it can be concluded that the model reduction can improve the accuracy of the yield prediction.

(d) Reduced weighted strategy with the overall effectiveness factors (200WREF)

In this strategy which was called 200WREF, the kinetic parameters in the reduced model (200WR) were estimated again whilst the overall effectiveness factors of lumps (η_j) were also estimated as model parameters. The resulted kinetic parameters and overall effectiveness factors are presented in TABLES 3 and 4, respectively. It is thought that the value of the estimated overall effectiveness factors were dependent to the transport specification of the lumps, discussed in the next section. The *AAD%*, R-squared and F-test of the model prediction were calculated and demonstrated with the title of 200WREF in the Figures 4, 5 and 6, respectively.

It can be understood from Figures 4, 5 and 6, 200WREF approach could improve the *AAD%* and R-squared of the prediction because of introducing the overall effectiveness factors in the model. Also, it can be seen that in comparison to 200WR strategy, the value of F-test has been decreased for the reason of entering four extra parameters in the model. It can be concluded that the effectiveness factors were less significant than the kinetic parameters. However, they had a positive effect to achieve better prediction.

TABLE 3 : Kinetic parameters for the 200WREF strategy.

Frequency Factor k_0 [$m^3.hr^{-1}.m^3\ cat^{-1}$]		Activation Energy E [kcal/mol]	
k_{0FD}	4.59×10^5	E_{FD}	15.94
k_{0Fk}	6.25×10^6	E_{Fk}	20.84
k_{0FHN}	-	E_{FHN}	-
k_{0FLN}	4.22×10^7	E_{FLN}	24.75
k_{0FG}	3.30×10^7	E_{FG}	24.12
k_{0DK}	1.19×10^9	E_{DK}	26.48
k_{0DHN}	-	E_{DHN}	-
k_{0DLN}	-	E_{DLN}	-
k_{0DG}	-	E_{DG}	-
k_{0KHN}	3.14×10^6	E_{KHN}	18.37
k_{0KLN}	-	E_{KLN}	-
k_{0KG}	-	E_{KG}	-
k_{0HNLN}	1.61×10^3	E_{HNLN}	7.53
k_{0HNG}	-	E_{HNG}	-
k_{0LNG}	2.32×10^1	E_{LNG}	-

TABLE 4 : Overall effectiveness factors of the hydrocracking lumps (200WREFstrategy).

Lump	Gen. effectiveness factor
Light Naphtha	0.988
Heavy Naphtha	0.745
Kerosene	0.947
Diesel	0.996
Un.VGO	0.998

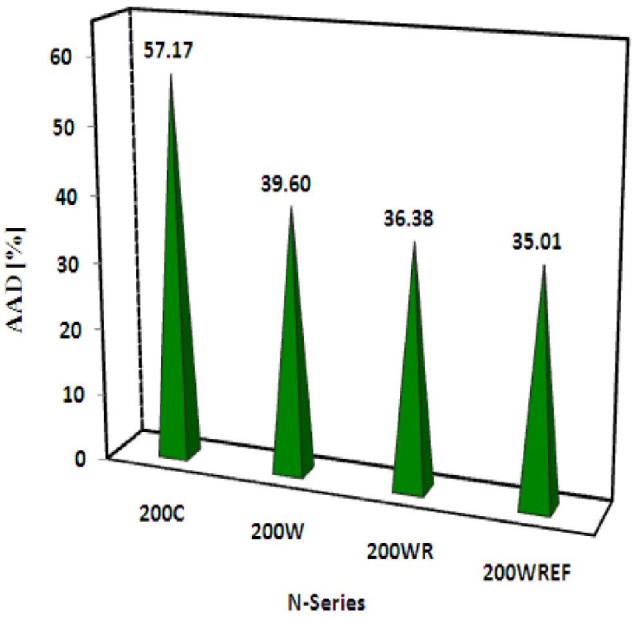

Figure 4 : The AAD% of the different strategies in the plug ideal- flow regime.

Full Paper

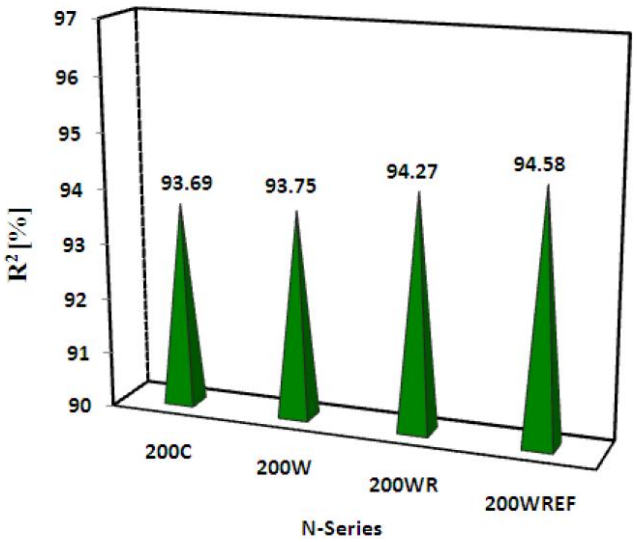

Figure 5 : The R-squared of the different strategies in the plug ideal- flow regime.

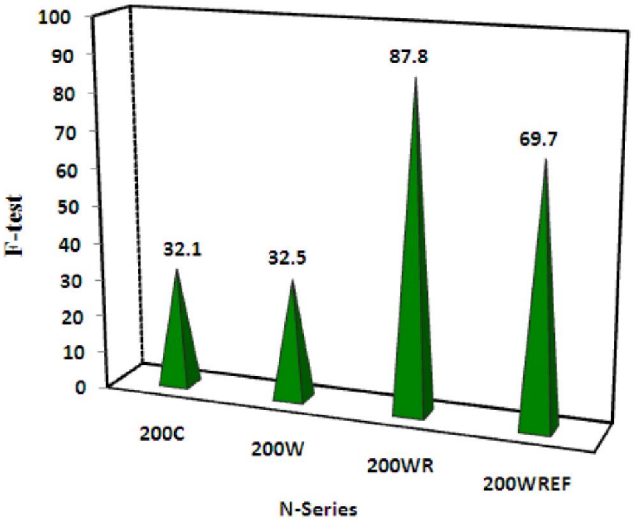

Figure 6 : The F-test of the different strategies in the plug ideal- flow regime.

Non-ideal flow regime

To simulate the effect of axial-dispersion on the hydrocracking reactions, N-series tank model was applied in which the number of series tanks (or cells) was decreased from N=200 to N=1, according to the Fibonacci golden numbers. The R-squared and F-test of the model prediction vs. number of tanks are demonstrated in Figures 7 and 8 respectively.

From Figure 7, It is observed that the R-squared of the prediction is improving gradually by decreasing the number of tanks up to N=13 (R^2=95.15%). Furthermore, from Figure 8, it can be seen that all points have lower F-value than the N=13. So this point was chosen because of better agreement between the experimental data and the predicted ones by the model. At this point, the *AAD%* of the prediction was decreased to 31.59%, which was about 4% lower than the best approach (200WREF) in plug flow regime (*AAD%*=35.01).

TABLE 5 : Kinetic parameters of the optimized series tanks model.

Frequency Factor k_0 [$m^3.hr^{-1}.m^3\ cat^{-1}$]		Activation Energy E [kcal/mol]	
k_{0FD}	4.59×10^5	E_{FD}	15.94
k_{0Fk}	6.25×10^6	E_{Fk}	20.84
k_{0FHN}	-	E_{FHN}	-
k_{0FLN}	4.22×10^7	E_{FLN}	24.75
k_{0FG}	3.30×10^7	E_{FG}	24.12
k_{0DK}	1.19×10^9	E_{DK}	26.48
k_{0DHN}	-	E_{DHN}	-
k_{0DLN}	-	E_{DLN}	-
k_{0DG}	-	E_{DG}	-
k_{0KHN}	3.14×10^6	E_{KHN}	18.37
k_{0KLN}	-	E_{KLN}	-
k_{0KG}	-	E_{KG}	-
k_{0HNLN}	1.61×10^3	E_{HNLN}	7.53
k_{0HNG}	-	E_{HNG}	-
k_{0LNG}	2.32×10^1	E_{LNG}	-

TABLE 6 : Overall effectiveness factors of the optimized series tanks model.

Lump	Gen. effectiveness factor
Light Naphtha	0.665
Heavy Naphtha	0.522
Kerosene	0.987
Diesel	0.929
Un.VGO	0.54
Average	0.728

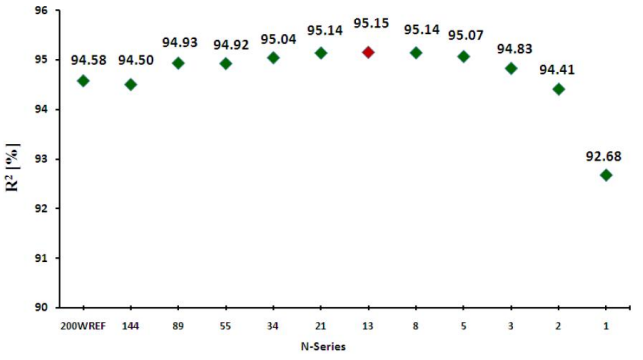

Figure 7 : The variation of the R-squared of the predicted yields vs. number of series tanks.

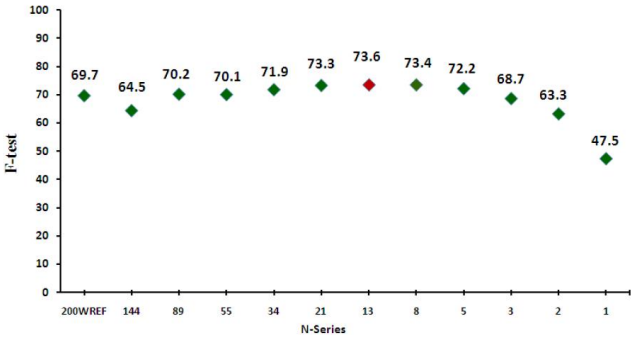

Figure 8 : The variation of the F-test of the predicted yields vs. number of series tanks.

TABLE 7 : Average yield, molecular weight and kinetic viscosity of lumps.

Lump	Average yield	Mw	υ (m^2/s)
Light Naphtha	0.056	85	4.7×10^{-7}
Heavy Naphtha	0.070	105	7.2×10^{-7}
Kerosene	0.186	165	1.91×10^{-6}
Diesel	0.241	230	7.67×10^{-6}
Un.VGO	0.351	450	2.79×10^{-5}

For the understudy reactor which was charged with 50 cm^3 catalyst (~10 cm length), non-ideal tanks-in-series approach indicated that because of axial-dispersion, the catalytic bed was divided to 13 perfectly mixed flow reactors each of which had 3.84 cm^3 volume and 0.77 cm length. It can be presumed that by following the presented strategy, the hydrodynamic behavior of the catalytic reactor was studied whilst the tracer (VGO) was not inert.

The estimated kinetic parameters for the optimized series tanks model (N=13) are tabulated in TABLE 5. It is clear that the value of activation energies were remained within the range of the reported values in the literature.

In TABLE 6, the estimated overall effectiveness factors for each lump engaged in the hydrocracking process are tabulated. From this table, it is found that the average value of the factors for all lumps is not far from the initial guess (0.8), reported in the literature. Additionally, it can be understood that kerosene and diesel have the highest factors, whilst heavy naphtha, unconverted VGO and light naphtha have the lowest ones, respectively. It was expected that light and heavy naphtha had the highest effectiveness factor because of their smaller and lighter molecules than the others. To have a better judgment, average experimental yields, molecular weight (Mw) and kinematic viscosity (υ) of lumps are tabulated in TABLE 7.

From TABLES 6 and 7, one can found that the introduced factors for each lump is dependent on average yield ($\overline{Y}_j$), molecular weight (Mw) and kinematic viscosity (υ) as

$$\eta_j = 7506.17\times(Y_j)^{1.246}\times Mw_j^{-1.325}\times\upsilon_j^{-0.011} \quad (22)$$

(R-squared=0.976)

The above relationship agrees with this concept that the lighter lumps, with lower molecular weights, have more ability (higher Knudsen coefficient) to diffuse inside the catalyst pores, whilst higher concentration (showed as yield) and lower kinematic viscosity increase the flux of the lumps which transfer from the bulk of the liquid to the surface of the catalyst. Consequently, it can be concluded that the overall effectiveness factors for this process were dependent to the both internal diffusion and external mass transfer resistances. Therefore the applied selective factors as model parameters, which were estimated from experimental data, could engage the model with transport phenomena in a simple and rational way to increase the model accuracy.

The parity diagrams for the measured data and the model predictions are presented in Figures 9 and 10. As revealed by these figured, the optimized series tanks approach including overall effectiveness factors gave an acceptable fit to experimental data.

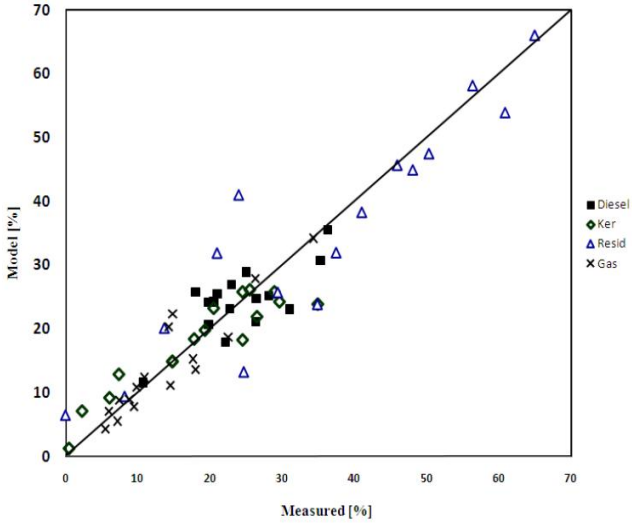

Figure 9 : Parity plot for gas, kerosene, diesel and residue resulted by optimized series tanks model.

Full Paper

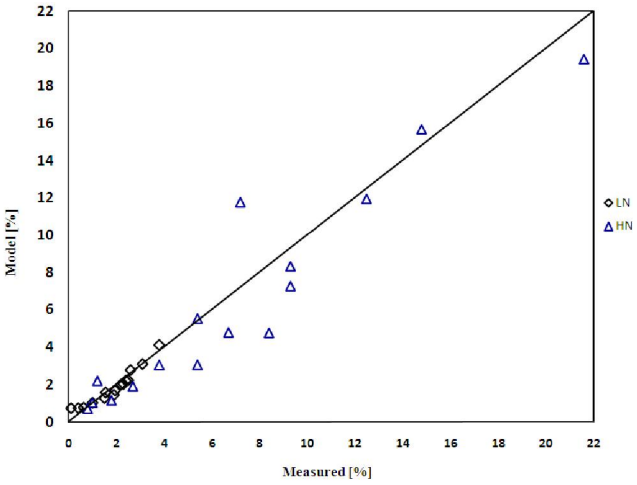

Figure 10 : Parity plot for light and heavy naphtha resulted by optimized series tanks model.

To summarize the discussion, in the TABLE 8, the ANOVA of all strategies (model parameters, summation of residuals, degree of freedoms, variance, F-test and F-critical) has been presented. The brilliant point in this table, is acceptable difference between F-critical and the F-test resulted by all models. Additionally, increasing the number of model parameters, which was resulted from importing selective overall effectiveness factors and N-series parameter to the model, ascended the F-test and descended the variance because of decreasing the error of residual.

TABLE 8 : Analysis of variance for different modeling approaches.

	200C	200W	200WR	200WRED	N-series
Model parameters	31	31	16	20	21
DF_{Reg}	30	30	15	19	20
DF_{Res}	65	65	80	76	75
S_{Res}	0.226	0.223	0.204	0.193	0.171
σ^2	3.48×10^{-3}	3.43×10^{-3}	2.55×10^{-3}	2.54×10^{-3}	2.28×10^{-3}
F-test	32.1	32.5	87.8	69.7	73.6
F-critical (DF_{Reg}, DF_{Res}, 1%)	2.39	2.39	3.09	2.67	2.61

CONCLUSIONS

A six-lump kinetic model involved of the selective overall effectiveness factors was developed to predict the product yields of a pilot scale vacuum gas oil hydrocracker. At first by using weighted lumping strategy and reducing the reaction network, the *AAD%*, R-squared and F-test of the prediction were improved from 57.17% and 93.69 to 36.38 and 94.27, respectively. Then, the effectiveness factors of the lumps were estimated like the kinetic constants, which led the *AAD%* and R-squared of the prediction to 35.01% and 94.58%, respectively.

Because of existing axial-dispersion through the catalytic bed, the tanks-in-series model was selected instead of the ideal plug flow one. Decreasing the number of tanks from N=200 (representing the plug flow) to N=1 (representing the mixed flow) according to the Fibonacci series, showed that thirteen series perfectly mixed tanks could decrease *AAD%* of the model to 31.59% as well as increase R-squared to 95.15%. Therefore, it was concluded that tanks-in-series approach could simulate the effect of the axial-dispersion in a hydrocracking reactor as if the R-squared of the model could be reached to higher than 95%, which could be acceptable for a kinetic base model.

Furthermore, the correlated relationship between the estimated overall effectiveness factors as a dependent variable to kinematic viscosity, molecular weight and concentration of lumps confirmed that lighter lumps, with lower molecular weight and kinematic viscosity had higher diffusivity whilst the concentration (showed as yield) increased the rate of diffusion. Therefore, by a simple approach, the effect of the internal resistance for pore diffusion, which was dependent to the molecular weight of lumps, and external resistance for the bulk diffusion, which was dependent to kinematic viscosity and concentration of lumps, were introduced to improve the yield prediction of the model.

REFERENCES

[1] K.Aboul-Gheit; Hydrocracking of vacuum gas oil (VGO) for fuels production, Erdol Erdgas Kohle, **105**, 1278-1284 **(1989)**.

[2] J.Ancheyta, F.Lopez, E.Aguilar; 5-lump kinetic model for gas oil catalytic cracking, Applied Catalysis A: General, **177**, 227-235 **(1999)**.

[3] J.Ancheyta, S.Sanchez, M.A.Rodriguez; Kinetic modeling of hydrocracking of heavy oil fractions: A review, Catalysis Today, **109**, 76-92 **(2005)**.

[4] K.Aoyagi, W.C.McCaffrey, M.R.Gray; Kinetics of hydrocracking and hydrotreating of coker and oil sand gas oils, Petroleum Sci.Technol., **21**, 997-1015 **(2003)**.

[5] R.Ayasse, H.Nagaishi, E.W.Chan; Lumped kinetics of hydrocracking of bitumen, Fuel, **76**, 1025-1033 **(1997)**.
[6] C.Botchway, A.K.Dalai, J.Adjaye; Kinetics of bitumen-derived gas oil upgrading using a commercial NiMo/Al_2O_3 catalyst, Can.J.Chem.Eng., **82**, 478-487 **(2004)**.
[7] M.A.Callejas, M.T.Martinez; Hydrocracking of a Maya residue, kinetics and product yield distributions, Ind.Eng.Chem.Res., **38**, 98-105 **(1999)**.
[8] G.M.Clarke, R.E.Kempson; Introduction to the design and Analysis of Experiments. London: Arnold, **(1997)**.
[9] R.A.Dunalp; The golden ratio and fibonacci numbers, World Scientific Publications, Houston, Texas, **(2003)**.
[10] J.H.Gary, G.E.Handwerk; Petroleum refining technology and economics, 4th Edition, Marcel Dekker Publication, **(2001)**.
[11] J.Govindhakannan; Modeling of a hydrogenated vacuum gas oil hydrocracker, Ph.D.dissertation: Texas Tech.University, **(2003)**.
[12] C.S.Hsu, P.R.Robinson; Practical advances in petroleum processing, 1st Edition, Springer, **1**, **(2006)**.
[13] G.Jing, Y.Jiang, M.H.Al-Dahhan; Modeling of trickle-bed reactors with exothermic reactions using call network approach, Chem.Eng.Sci., **63**, 751-764 **(2008)**.
[14] R.Krishna, A.K.Saxena; Use of an axial-dispersion model for kinetic description of hydrocracking, Chem.Eng.Sci., **44**, 703-712 **(1989)**.
[15] A.Kumar, G.M.Ganjyal, D.Jones, M.A.Hanna; Modeling residence time distribution in a twin-screw extruder as a series of ideal steady-state flow reactors, J.of Food Eng., **84**, 441-448 **(2008)**.
[16] O.Levenspiel; Chemical reaction engineering, 3rd Edition, John Wiley & Sons Inc., **(2001)**.
[17] G.Mary, J.Chaouki, F.Luck; Trickle-bed laboratory reactors for kinetic studies, International J.Chem. Reactor.Eng., 7 **(2009)**.
[18] E.M.Matos, R.Guirardello; Modeling and simulation of the hydrocracking of heavy oil, fractions, Braz.J.Chem.Eng., **17**, 1 **(2000)**.
[19] R.A.Meyers; Handbook of petroleum refining processes, 2nd Edition, New York, McGraw-Hill, **(1986)**.
[20] P.L.Mills, M.P.Dudukovic; A dual-series solution for the effectiveness factor of partially wetted catalysts in trickle-bed reactors, Ind.Eng.Chem.Fund., **18**, 2 **(1979)**.
[21] S.Mohanty, D.N.Saraf, D.Kunzro; Modeling of a hydrocracking reactor, Fuel Processing Technology, **29**, 1-17 **(1991)**.
[22] D.C.Montgomery; Design and analysis of experiments. New York: John Wiley & Sons, **(2001)**.
[23] F.Mosby, R.D.Buttke, J.A.Cox, C.Nikolaids; Process characterization of expanded-bed reactors in series, Chem.Eng.Sci., **41**, 989 **(1986)**.
[24] V.K.Pareek, Z.Yap, M.P.Brungs, A.A.Adesina; Particle residence time distribution (RTD) in three-phase annular bubble column reactor, Chem.Eng. Sci., **56**, 6063-6071 **(2001)**.
[25] K.Sertic-Bionda, Z.Gomzi, T.Saric; Testing of hydrosulfurization process in small trickle-bed reactor, Chem.Eng.J., **106**, 105-110 **(2005)**.
[26] S.Sadighi, A.Ahmad, S.R.Mohaddecy; 6-lump kinetic model for a commercial vacuum gas oil hydrocracker, Int.J.Chem.Reactor Eng., 8 **(2010a)**.
[27] S.Sadighi, A.Arshad, A.Irandoukht; Modeling a pilot fixed-bed hydrocracking reactor via a kinetic base and neuro-fuzzy method, Journal of Chemical Engineering Japan, **43(2)**, 174-185 **(2010b)**.
[28] S.Sadighi, A.Ahmad, A.Irandoukht; Kinetic study on a commercial amorphous hydrocracking catalyst by weighted lumping strategy, Int.J. Chem.Reactor Eng., 8 **(2010c)**.
[29] S.Sanchez, M.A.Rodriguez, J.Ancheyta; Kinetic model for moderate hydrocracking of heavy oils, Ind.Eng.Chem.Res., **44(25)**, 9409-9413 **(2005)**.